

Supplementary Material: Biosolids leachate variability, stabilization surrogates, and optical metric selection

Sarah Fischer,^{a,b,*} Michael Gonsior,^c Jon Chorover,^d Leanne Powers,^{c,f} Amanda Hamilton,^b
Mark Ramirez^e, and Alba Torrents^{a,c}

^aMarine, Estuarine, and Environmental Sciences Program, University of Maryland, College Park, MD 20742

^b Department of Civil and Environmental Engineering, University of Maryland, College Park, Maryland.

*Corresponding Author, sjfischer@missouri.edu, Current address: Civil and Environmental Engineering Department, University of Missouri, Columbia.

^b University of Maryland Center for Environmental Science, Chesapeake Biological Laboratory, 146 Williams Street, Solomons, MD 20688, USA

^d Department of Soil, Water and Environmental Science, University of Arizona, 1177 E 4th St., Tucson AZ 85721, USA

^eDistrict of Columbia Water and Sewer Authority (DC Water) Blue Plains, 5000 Overlook Avenue, Washington, District of Columbia

^f Department of Chemistry, SUNY College of Environmental Science and Forestry, Syracuse, NY 13210

SI Section 1: Methods and Results for Total and Volatile Solids, Dissolved Organic Matter (DOM) Extraction, DOC, and pH measurement

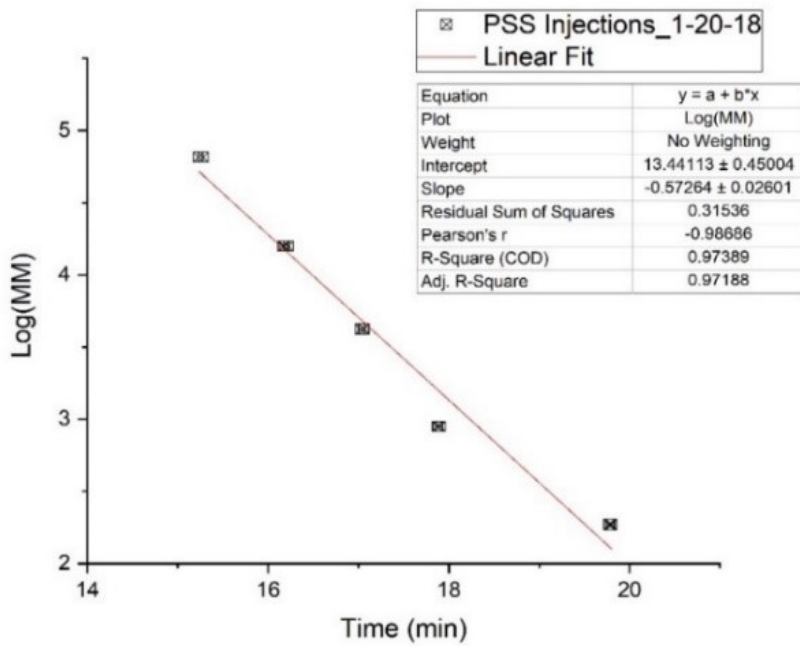
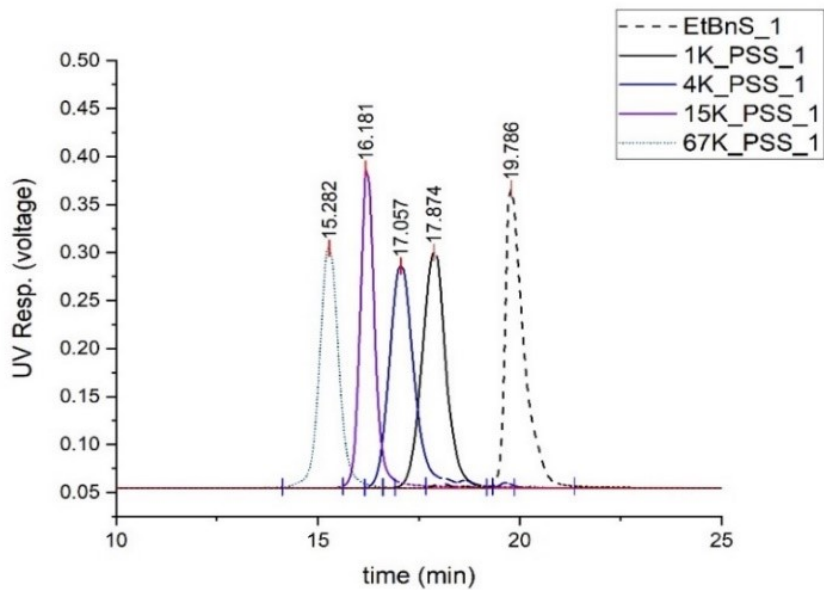
The total solids (%TS) of biosolid grab samples was determined by precisely measuring wet solids and drying samples at 105°C for a minimum of 12 hours, cooling, and reweighing of dry matter following EPA Method 1684. Volatile solids (%VS) of dried residues were then determined by ignition at 550°C for 2 hours, then cooling and reweighing. Water-extractable DOM was extracted from biosolids with deionized water in a 1:10 w/v solid:water ratio on an orbital shaker at room temperature for 24 hours.^{1,2} Suspensions were centrifuged at 10,000 rpm and the supernatant was filtered with a 0.45 µm cellulose acetate membrane filter (Whatman GD/X).

Suwannee River Natural Organic Matter (SRNOM, Lot 2R101N) was obtained from the International Humic Substances Society and characterized as a reference material (IHSS) throughout the study. Stock solutions of SRNOM were prepared by dissolution into ultrapure deionized water, sonication, and filtration by 0.45 CA membrane filters also used for biosolid leachates. Treatment train sludge samples with high water (95%) were centrifuged directly and then filtered. DOC of extracts was determined as non-purgeable organic carbon via a platinum oxidation catalyst and non-dispersive infrared gas analyzer (Shimadzu TOC/TN-L, Columbia, MD). The instrument was calibrated with a freshly-made glycine standard curve and with repeat testing of standards as unknown to assess drift and reproducibility. DOC of each sample was analyzed with repeated injections to meet the criteria that coefficient of variation for peak areas was less than 2% per sample.

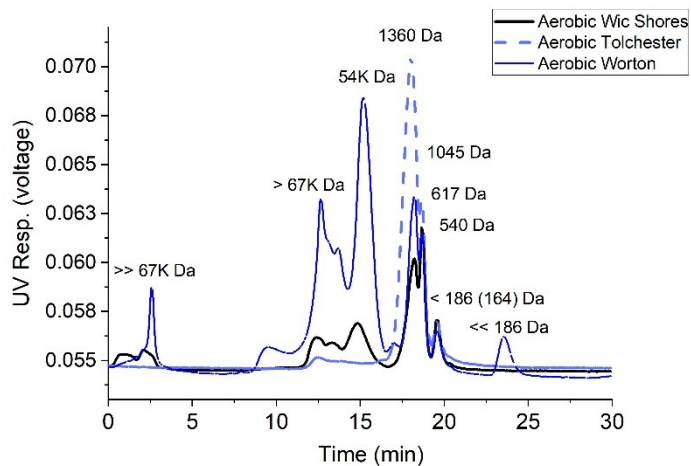
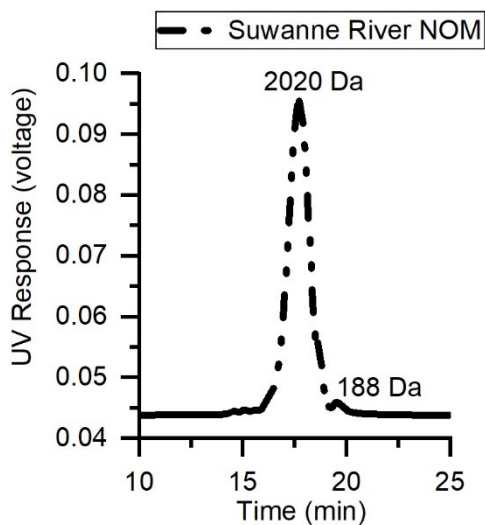
The pH of biosolids-DOM extracts was measured with an Orion Star A211 meter and Mettler Toledo LE409 pH probe, calibrated with low ionic strength buffer, as the ionic strength of DOM extracts was well-below low ionic strength calibrants.

SI Section 2: Methods and Additional Results of High Performance Size-Exclusion Chromatography of Biosolids Extracts

Apparent molar mass distributions in biosolids-DOM samples were determined with high pressure liquid chromatography size-exclusion chromatography (HPLC-SEC) using an Agilent 1200 Series HPLC (Santa Clara, CA) with a photodiode array (PDA) detector operating at 280 nm at the Arizona Lab for Emerging Contaminants (Tucson, AZ). Two stainless steel (8 x 300 mm) SEC columns (MCXGPC 1000 and 100,000 Å, PSS Polymer Standard Service-USA, Inc Amherst, MA) were connected in series, equipped with a guard column. Standards of polystyrene sulfonate (PSS-Polymer Standard Service-USA) with nominal molar masses ranging from 1 to 67 kilodaltons (kDa) and a low molecular mass 4-ethylbenzenesulfonic acid (186 Da) standard, all at ~2.5 mg/mL, were utilized for a linear calibration of log (molar mass) to column retention time.³⁻⁵ Aquatic DOM reference material Suwannee River Natural Organic Matter (SRNOM, Lot 2R101N) was obtained from the International Humic Substances Society and characterized as a reference material (IHSS). All standards, samples, and reference materials were brought to a concentration of 30 mg C L⁻¹ and adjusted to a pH ~7.4 in a 20 mM sodium phosphate buffer solution prepared with nanopure water. The 20 mM phosphate buffer was also the mobile phase for isocratic HPLC-SEC runs. Samples and standards were injected at 50 µL and a flow rate of 1 mL/min. The linear relationship between standards log molar mass (MM) and retention time was $\text{Log}(\text{MM}) = -0.572 (\text{min}) + 13.4 \pm 0.45$, adj. R-square = 0.97. Peak retention times were identified with Origin Lab software. This retention time was converted to apparent, peak molar mass (M_p) by the linear relationship of standards log(MM) to retention time.



SI Figure 1: SEC chromatogram for 67K-182 Da standards, retention times (min) labeled above peaks. Standards were injected in triplicate. b. Resulting calibration curve of PSS Standards Retention times versus Log(Molar Mass). The linear relationship between standards log molar mass (MM) and retention time was $\text{Log}(\text{MM}) = -0.57264(\text{min}) + 13.44113 \pm 0.45004$, with an adj. R-square = 0.972. Error bars represent average RT of triplicate injections per molar mass standard; error bar magnitude was smaller than the point size displayed.



SI Figure 2: Chromatogram of aquatic isolate Suwanee River Organic Matter reference material (left). Apparent molar mass of peak (M_p) locations are indicated in Daltons (Da) . Majority of SROM corresponded to an M_p of 2020 Da with small signal corresponding to 188 Daltons. d. Full chromatogram of AeD-biosolids DOM and evidence of particulates, polymer, and/or supramolecular assembly.

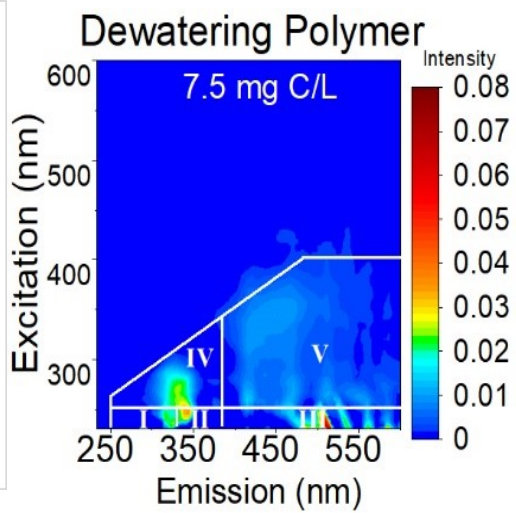
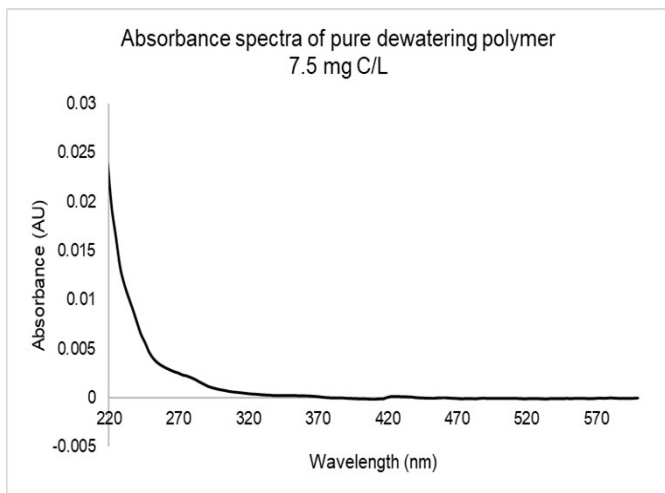
SI Section 3: Detailed results of optical spectra and optical metric calculations

Absorbance spectra and excitation emission matrices (EEMs) of biosolids-DOM were measured for multiple RRFs and dates. Optical properties of dewatering polymer was also assessed.

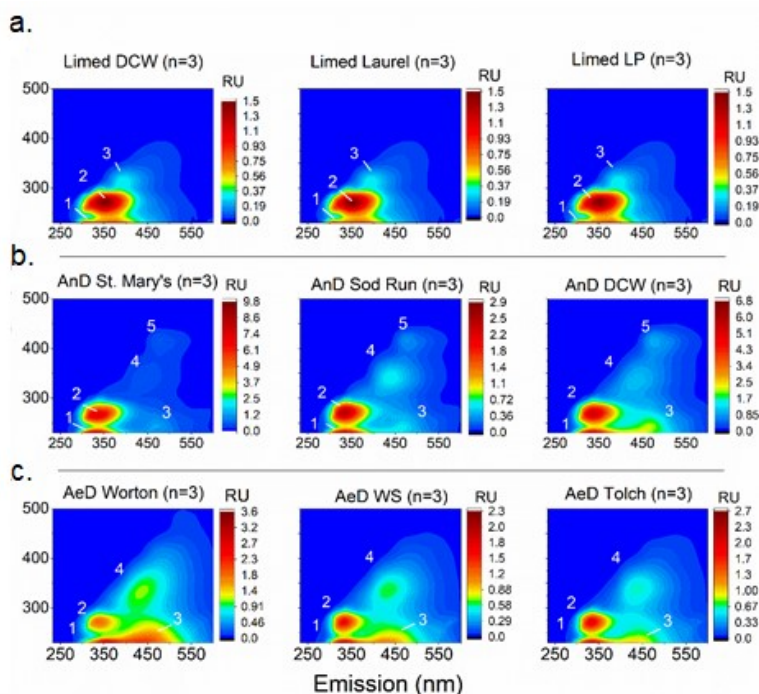
a.



b.



SI Figure 3: a) Filtered sludge leachates. Leachates from the Worton, MD facility were blue in color. (b) Absorbance and fluorescence EEM spectra of proprietary dewatering polymer added to sludge before final dewatering. Optical spectrum of pure dewatering polymer was assessed at 7.5 mg C/L. Polymer is added to sludge at a 2.5% volume polymer: volume sludge (personal correspondence, DCWASA). Via the absorbance and fluorescence intensity, polymer is expected to contain minimal fluorescence contribution (>0.08 RU) to sludge-FDOM.



SI Figure 4: Excitation emission matrices (EEMs) of biosolids-DOM from multiple RRFs and stabilizations. EEMs presented were averaged for $n=3$ sampling dates and three extractions per solid. Table 1 describes the nine facilities sampled. Row a) presents biosolids leachates from lime treated (LT) materials, row (b) indicates anaerobically digested (AnD) biosolids leachates, and row (c) indicates and aerobically digested (AeD) leachates from three target facilities. Fluorescence maxima were identified and numbered, and fluorescence intensity is displayed as Raman Units (RU).

Computation for Fluorescence Regional Integration (FRI)

The fluorescence EEMs of replicate DOM extracts (n=3 per 9 RRFs) was individually integrated for five previously described regions; (I) “tyrosine-like”, (II) “tryptophan-like”, (III) “fulvic acid-like”, (IV) “microbial by-product-like, and (V) “humic acid-like” (Chen et al., 2003, SI Table 1). Following Chen et al. (2003) and others, the total volume (Φ_i) of each region of the EEM boundaries is summated by:

$$\Phi_i = \sum_{\lambda_{Ex}} \sum_{\lambda_{Em}} I(\lambda_{Ex}, \lambda_{Em}) \Delta\lambda_{Ex} \Delta\lambda_{Em} \quad (\text{Eqn. 1})$$

where $\Delta\lambda_{Ex}$ is the excitation wavelength interval, $\Delta\lambda_{Em}$ is the emission wavelength interval and $I(\lambda_{Ex}, \lambda_{Em})$ is fluorescence intensity at each excitation-emission wavelength pair. The total number of data points for each region were computed to produce the fractional projected excitation-emission factor (F_i). The normalized fluorescence intensity volume (Φ_{in}) beneath region of the DOM sources was then computed:

$$\Phi_{in} = F_i \Phi_i \quad (\text{Eqn. 2})$$

The fluorescence percentage of each region is calculated by the ratio of normalized regional volume to total FRI volume:

$$P = \Phi_{in} / \Phi_{T,n} * 100\% \quad (\text{Eqn. 3})$$

Where ($\Phi_{T,n}$) is sum of all normalized fluorescence of all regions. The final fluorescent region percentages (P) for each EEM was averaged by solid stabilization type. Standard deviation of P

regions were computed based on multiple EEM FRI analysis per stabilization. Volume of each regions were summated with equations 1-3.

SI FRI Table: Excitation and emission (Ex/Em) wavelength boundaries applied for fluorescence regional integration (FRI) analysis of biosolids-dissolved organic matter extracts. Based on classically defined boundaries by Chen et al. (2003).

Region	Description	Ex/Em wavelength boundaries (nm)
I	Tyrosine-like protein	230–250/233–330
II	Tryptophan-like protein	230–250/330–380
III	Fulvic acid-like organics	230–250/380–600
IV	Soluble microbial by-product	250–340 diagonal/260–380
V	Humic acid-like organics	250–340, 340-400 diagonal /380–600

SI Table 1: Absorbance metric definitions, references, and results of biosolid leachates by treatment type.

Definitions and results	SUVA ₂₅₄	E ₂ /E ₃	Spectral Slope S ₂₇₅₋₂₉₅	Slope Ratio S _R
Calculation	The specific UV absorbance at 254 nm normalized to DOM concentration	Ratio of UV absorbance at 250 nm to 364 ⁶ nm	Nonlinear fit of an exponential function to the absorption spectrum over the wavelength range	Spectral slope S ₂₇₅₋₂₉₅ divided by spectral slope S ₃₅₀₋₄₀₀
Interpretations	SUVA ₂₅₄ is frequently used as a proxy for the overall degree of DOM aromaticity due to the absorptivity for absorbance light by aromatic compounds	Decreasing E ₂ /E ₃ values reflect that the DOM matrix has a higher average molecular weight	Proxy for Molecular Weight changes in a broad range of samples. Independent of carbon concentration	Negatively correlated to DOM molecular weight. Independent of carbon concentration.
Reference	Weishaar et al. ⁷	Peuravouri and Pihlaja ⁸	Helms et al. ⁹	Helms et al. ⁹
Limed Biosolids DOM	1.33 ± 0.23	21.08 ± 7.89	0.05 ± 0.01	1.56 ± 0.67

n= 12				
Aerobic Digested DOM n = 11	2.41± 1.24	9.91 ± 7.89	0.02 ± 0.01	1.18 ± 0.76
Anaerobic Digested DOM n = 12	2.77 ± 1.08	7.24 ± 2.35	0.03 ± 0.01	2.77 ± 1.08

SI Table 2: Fluorescence Indices and definitions. Fluorescence indices were computed on individual EEMs and averaged by treatment type. Standard deviation of averages of treatment type are also reported.

	Humification Indices (z, o): zHIX oHIX	Modified Biological Index BIX	Fluorescence Index: FI
Calculation	At fixed Ex: 254 nm z: ratio of area under (Em: 435–480 nm)/ Area under (Em 300–345 nm) o: ratio of area under (Em: 435–480 nm)/ Sum (Area under +(Em: 435–480 nm) and (Em 300–345 nm))	Ratio of signal at Em: 380 n.m. /430 n.m., at Ex: 310 nm Ratio of β/α emission at fixed wavelength. Modified as $\beta = 380$ n.m. $\alpha = 430$ n.m	Ratio of signal at Em: 470 nm/em 520 nm at Ex 370 nm.
Interpretation	Higher numbers previously indicated lower H/C ratios shifting the emission to longer wavelengths and a greater degree of humification. Developed with soil extracts.	Increase in BIX suggests autochthonous production or microbial input to humic substances of aquatics and marine systems	Precursor material for DOM is of a more microbial (FI ~1.8) in nature or more terrestrially derived (FI ~1.2).
Reference	o = Ohno (2002) z = Zsolnay et al. (1999)	Parlanti et al. (2000) Huguet et al. (2009)	McKnight et al. (2001)
Limed Biosolids DOM n= 12	z: 0.41 ± 0.18 o: 0.28 ± 0.09	1.70 ± 0.62	2.15 ± 0.14
Aerobic Digestion: n = 11	z: 1.08 ± 0.46 o: 0.50 ± 0.10	0.67 ± 0.1	2.01 ± 0.08
Anaerobic Digestion: n = 12	z: 0.75 ± 0.52 o: 0.37 ± 0.16	0.81 ± 0.19	2.24 ± 0.24

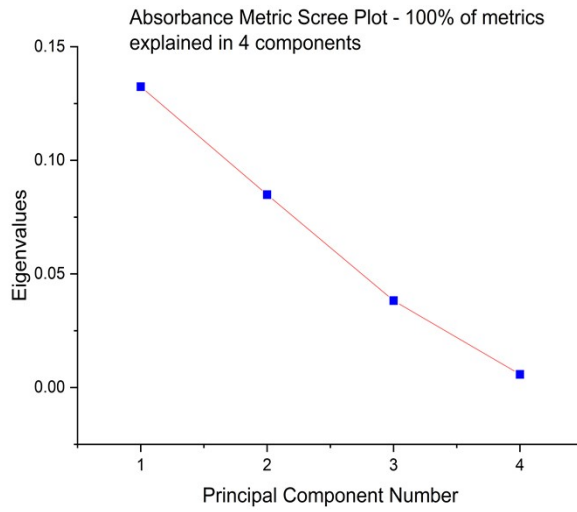
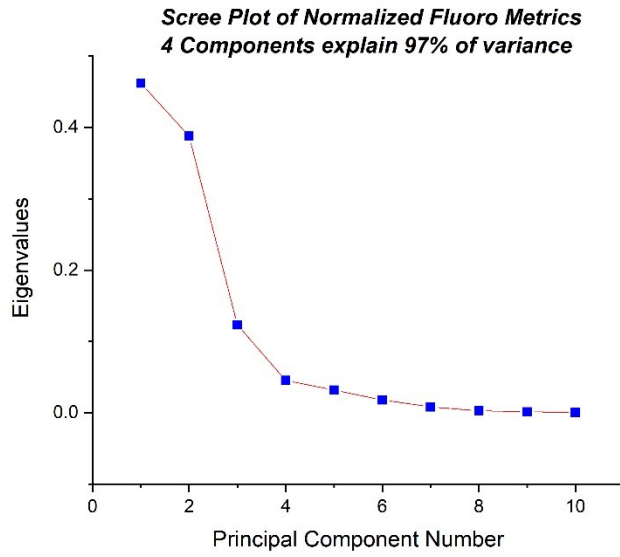
SI Table 3: Fluorescent (FDOM) Component Peaks areas summarized in Stedman et al.¹⁰, Coble et al.¹¹, Gabor et al.¹², and Korak et al.¹³

Peak	Potential Fluorophore Type, considering source as well	Ex (nm) Range	Em (nm) Range
B	Tyrosine-like protein	260-290	300-320
T	T ₁ , Tyrosine-like, protein-like (T ₂ for phenolic sources, Maie et al. 2007)	260-290	326-350
A	UV Region Humic-like and fulvic acid-like	240-270	380-470
C	Visible Humic-like	300-340	400-480

SI Table 3.1: Determination A:C and T:C Peak ratios by classically defined boundaries and difference to proximal maxima of biosolids DOM, peak T:C ratio and was also computed.

Computation, Reference, and Interpretation:	Ratio of Peak A:C Maxima, Classically Defined	A:C Ratio adapted for proximal maxima to A:C	Ratio of Peak T:C Maxima, Classically Defined	Adapted Ratio of Biosolids-DOM Proximal Maxima to T:C
Coble et al. 1996 UV:Visible Humics		Value and Difference to Classic Ratio (%)	Baker et al. 2002: Protein-like:Fulvic-like	Value and Difference to Classic Ratio Indicated (%)
LT Biosolids DOM (n= 12)	1.2	1.5 (20.1%)	1.7	1.5 (12%)
AeD Biosolids DOM: (n = 11)	1.8	1.9 (6.4%)	2.3	2.3
AnD Biosolids DOM: (n = 12)	2.3	2.4 (5.3%)	5.1	5.1
Suwannee River Natural Organic Matter	2.2	2.4	Not Applicable to SRNOM Low fluorescence in T region	Not Applicable to SRNOM

1. Principal Component Analysis (PCA) of optical metrics for distinguishing biosolid leachates by treatment



SI Figure 6: Scree Plots and Principal Component Analysis (PCA) absorbance and fluorescence metrics together. Top: Scree Plot of normalized optical metrics indicated that a four component model significantly explained 97% of variance and was chosen for the covariance loading and biplot. **(b)** Covariance loading and biplot of optical metrics. Samples clustered by treatment but there was significant overlap between absorbance and fluorescence metrics. Absorbance and fluorescence metrics were separated in additional PCAs.

Additional Fluorescence Spectroscopy of Sludge-DOM across Solid Stabilization trains

Primary sludge influent to digesters was dominated by UV fluorescence (1 & 2) and digested DOM and final biosolids extracts contained additional fluorescence in humic and fulvic-acid associated regions. Peak ratios are computed in

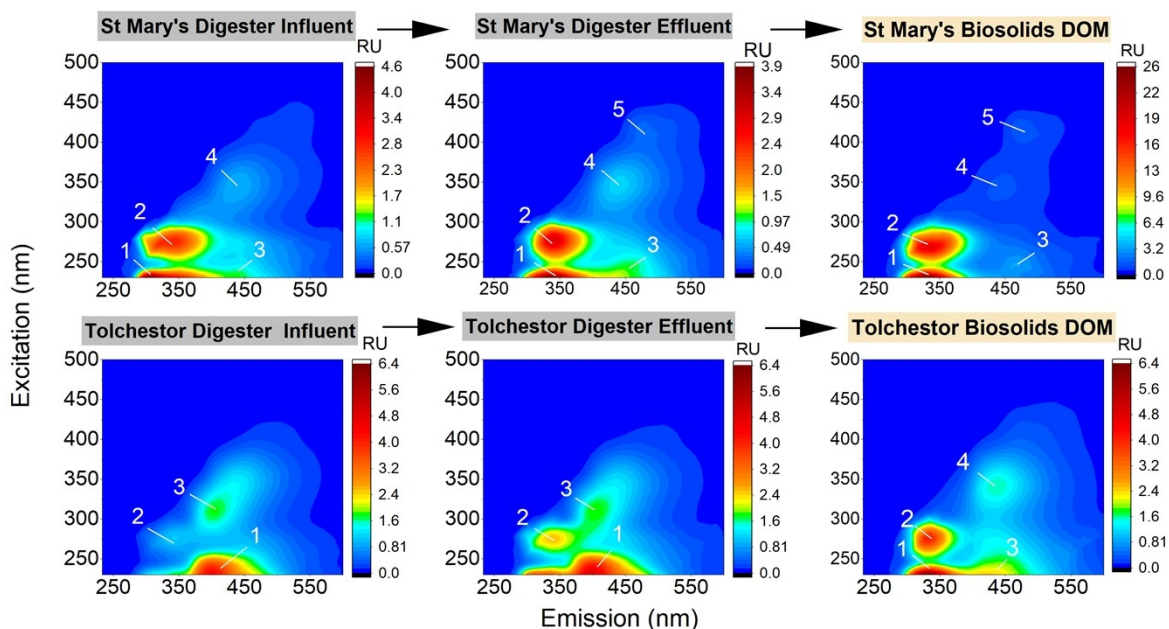
SI Table 4: Peak ratio values for sludge treatment trains shown in Figure 5, Main text:

AnD Treatment Train – THP system	B:A	B:C	A:C	U:B	U:A	U:C
1. Influent to thermal hydrolysis pretreatment (THP)	Only Peak B Present	---				
2. Post THP, Influent to anaerobic digestion	0.73	1.37	1.87	N/A	NA	NA
3. Final Biosolids-DOM	1.26	2.89	2.30	0.33	0.41	0.95
AnD Treatment Train – without THP system	B:A	B:C	A:C	U:B	U:A	U:C
1. Influent to AnD (post fermentation)	Peak B only	--	--			
2. AnD Effluent	1.10	0.99	0.89			
3. Final Biosolids-DOM	3.82	3.92	1.02	0.14	0.55	0.57

FDOM transformations across additional treatment trains of the St. Mary’s facility (AnD) and Tochester, MD facility (AeD) were less pronounced than (Figure 7, SI Figure 7). Fluorophore composition shifted or changed intensity, but heterogenous red-shifted fulvic acid-like to humic acid like maxima were present before digestion. Fluorophore maxima > 400 nm appeared to

develop after digestion. Less pronounced transformations in some treatment trains may be due to the influence of previously solubilized and dissolved carbon.

SI Figure 7: Fluorescence spectroscopy of two additional AnD and AeD treatment trains: St. Mary's (St M.) and Tolchester, MD (Tolch) facilities.

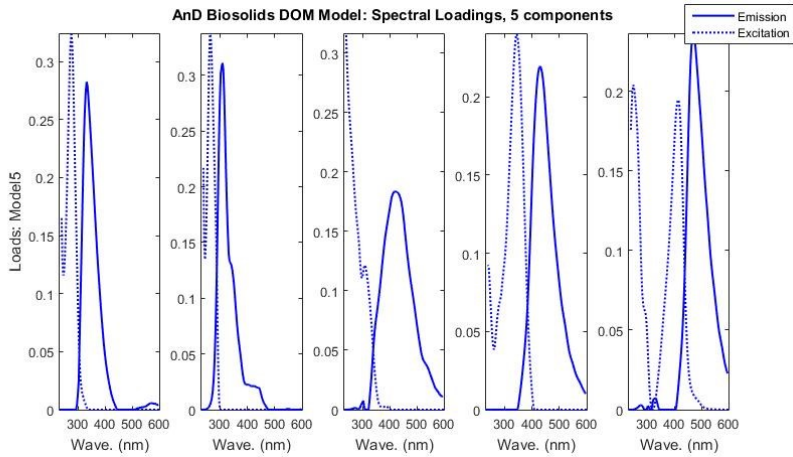
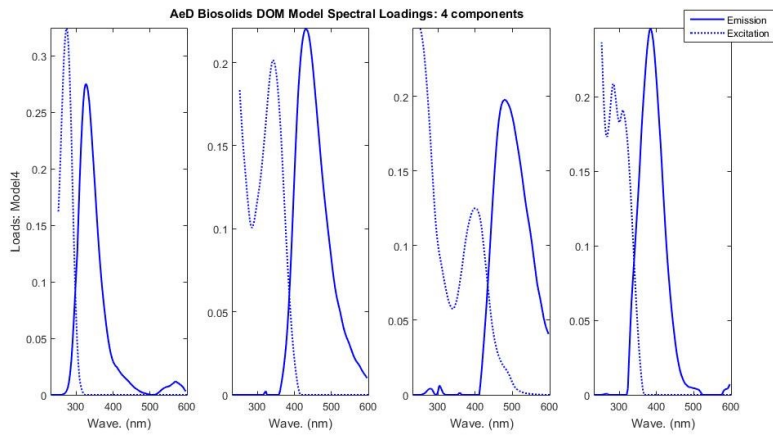
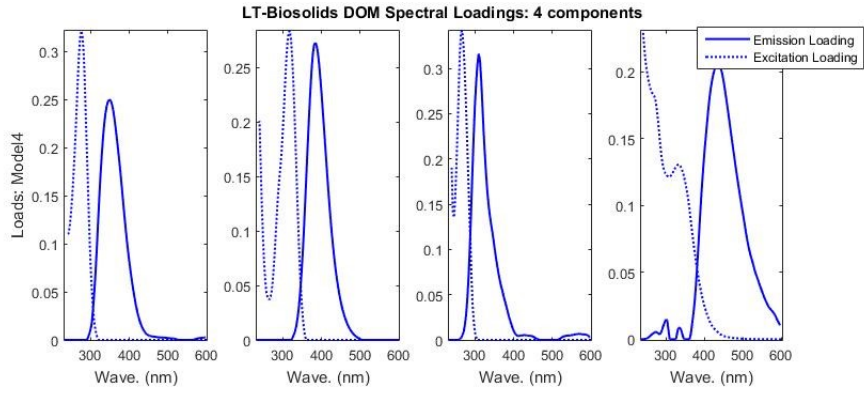


2. PARAFAC Model Development and Comparisons in the OpenFluor Database

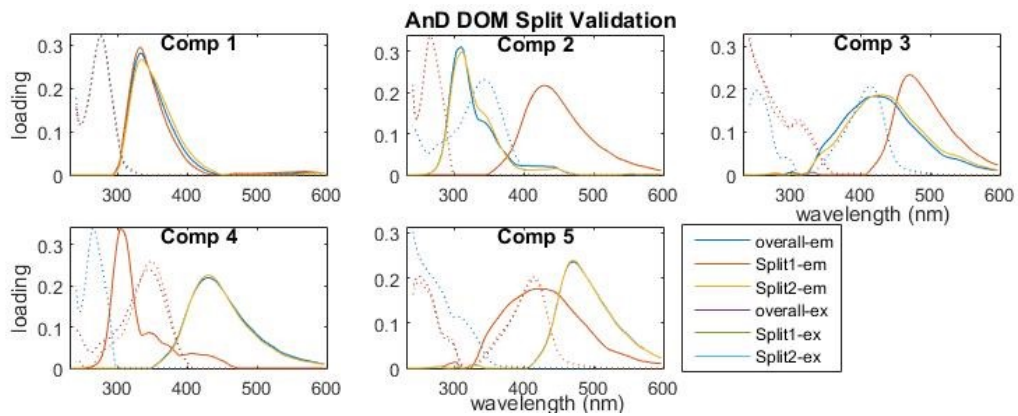
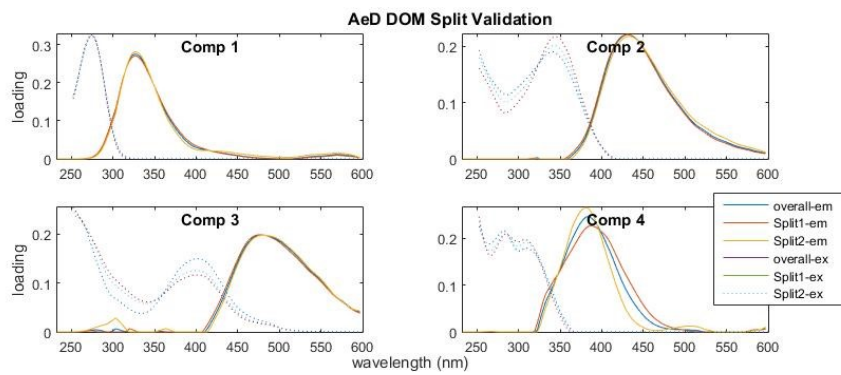
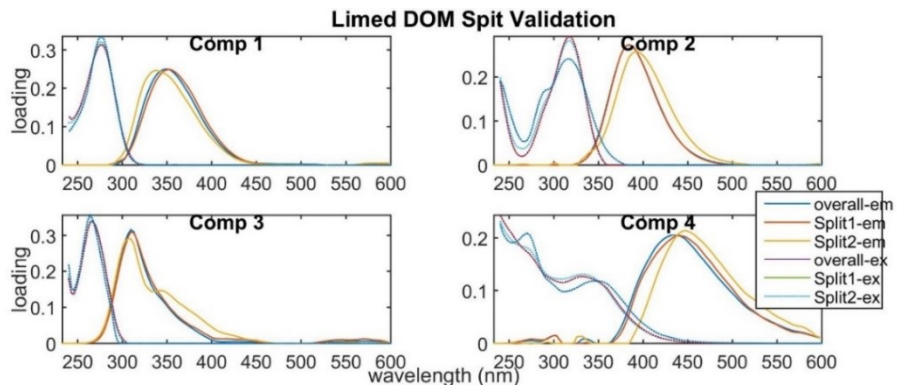
PARAFAC models were developed with the drEEM 1.0 toolbox following the procedures described in detail by Murphy et al. (2013) for Matlab® (MathWorks; Natick, MA).

EEMs were modeled by treatment type with 3-4 extractions and fluorescence measurements per RRF solid and at least three RRFs per stabilization category. Limed solids were modeled via $n = 12$ EEMS, AeD solids were modeled with $n = 11$ EEMs, and AnD solids were modeled $n = 12$ EEMs. PARAFAC models were built for each treatment type individually because treatment types yielded fundamentally different fluorophore compositions and locations in qualitative assessment. Targeted model development can avoid issues with over-fitting EEMs (Mostofa et al. 2019). Input data was preprocessed according to best practices recommended by Murphy et al. (2013) and normalized before preliminary analyses. EEMs spanned Ex:Em ranges of 240–597 nm and 233-600 nm. Exploratory analyses of excitation and emission loadings confirmed that a four-component model was best suited for LT and AeD-biosolids DOM models and a five-component model was appropriate for AnD-biosolids DOM (Figure S2 of supporting information). A convergence criterion of 10^{-8} was used for the three models and model convergence was confirmed with 60 to 120 random iterations. All data was reverse-normalized at the end of the analysis following Murphy et al. (2013). Split-half analysis validated the three models through data split comparison with alternating sample distribution (SI Figure 3). PARAFAC models were also deposited to the OpenFluor database (www.openfluor.org). Results of Biosolid-DOM models compared to previously submitted DOM PARAFAC models in the database are shown for a 0.97 similarity threshold (SI Figure 5).

The three biosolids PARAFAC models developed were deposited in the OpenFluor database (www.openfluor.org) will be made publicly available after publication. The PARAFAC models will also be available for direct downloads via the Dryad platform (<https://datadryad.org/>) and additional sludge-DOM EEMs could be amended to PARAFAC models to assess differences and similarities from the three models proposed.



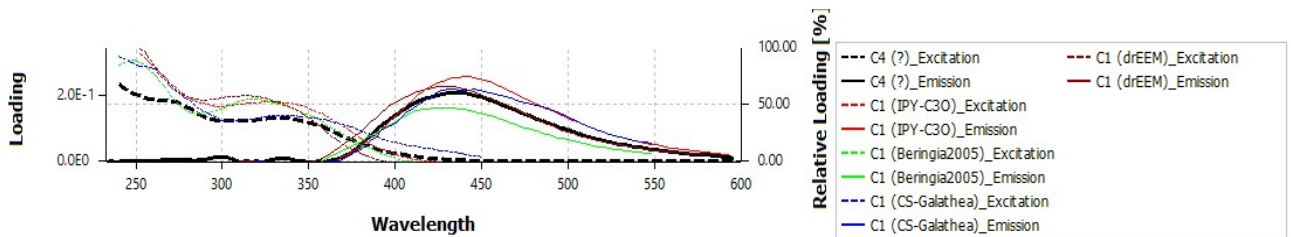
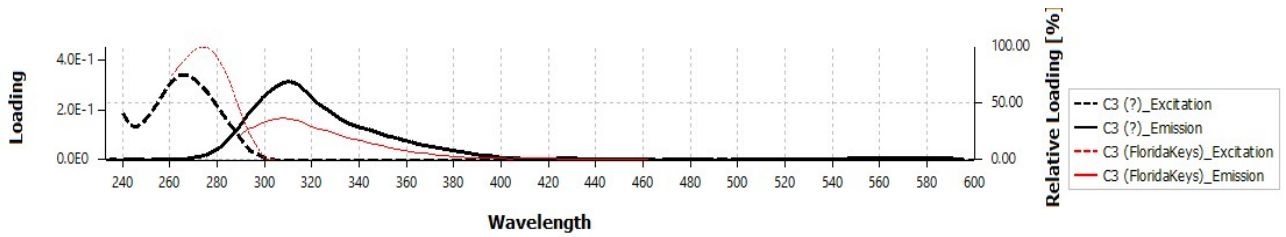
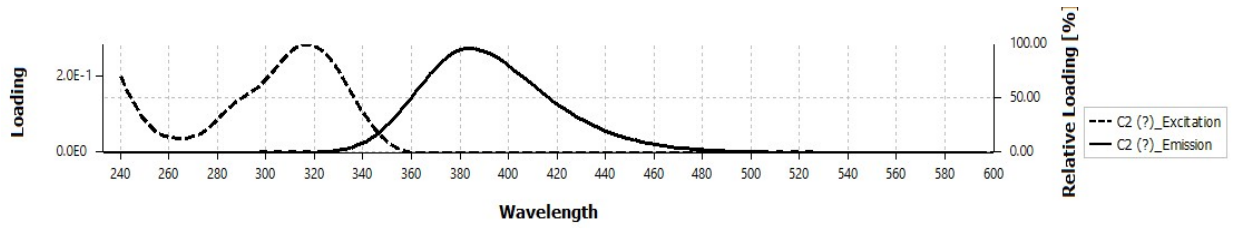
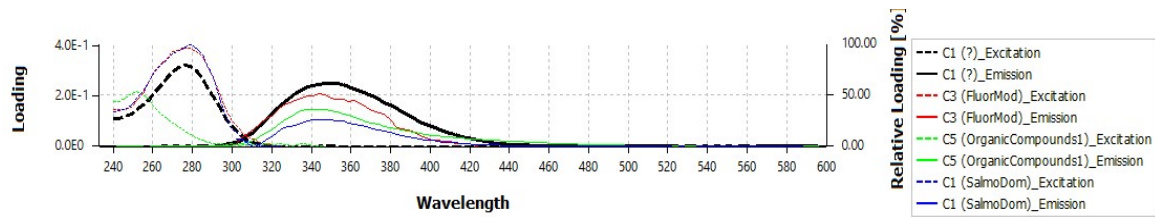
SI Figure 8 a.: Excitation and emission loadings of 4 and 5 component EEM-PARAFAC models generated during preliminary analysis. Loadings were appraised for the following features (Murphy et al. 2013): (i) minimal overlap between the excitation and emission spectra, (ii) excitation spectra that may have multiple peaks, but emission spectra exhibit a single distinct peak, (iii) excitation spectrum has two or more peaks indicating consecutive excited state absorption bands, some absorption (excitation) occurs between these peaks, and (iv) excitation and emission spectra do not exhibit abrupt changes over very short wavelength distances.



SI Figure 8 b.: Split Half Validations of PARAFAC Models

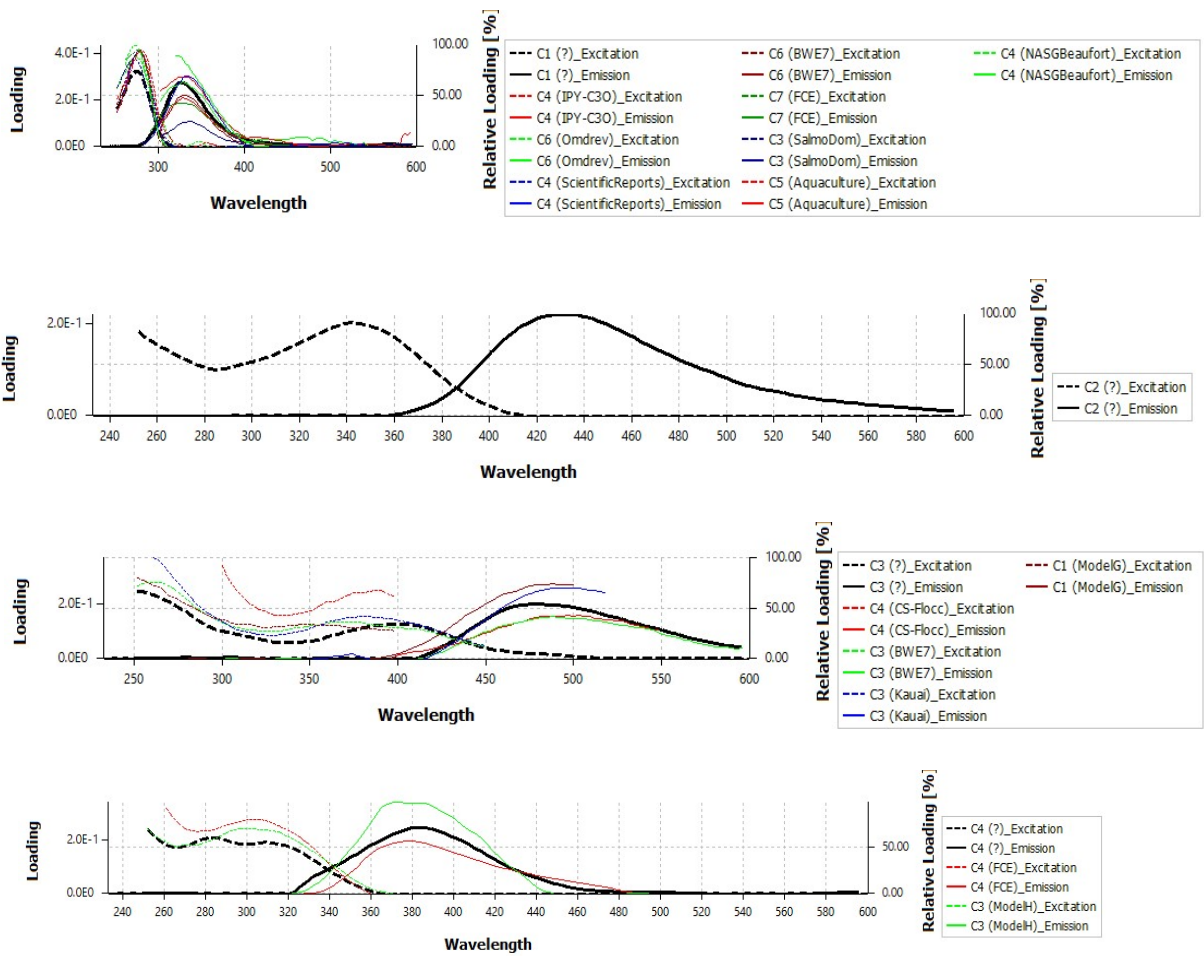
SI Figure 9: Component comparisons at a 0.97 threshold for three biosolids-DOM PARAFAC models deposited to the OpenFluor plugin for OpenChrom. Three models (a.,b., and c.) are presented for each treatment:

- a. Model Name: **Limed Digestion**



Matched Models: 8 / 70, Min, Min Similarity Score: 0.97, Software: OpenFluor plugin for OpenChrom Version: 1.3.0.2017101902, Matched Components (Excitation/Emission)

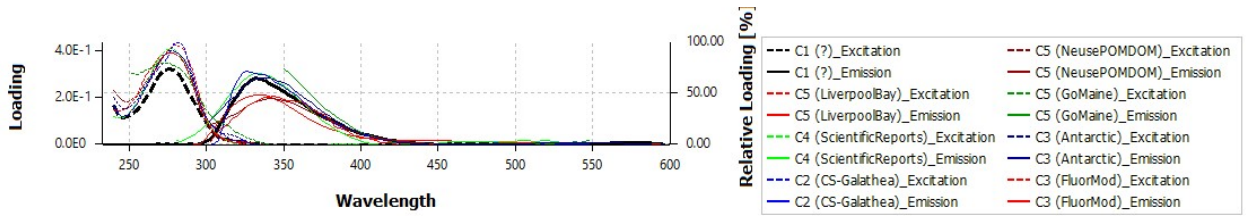
b. Model Name: **Aerobic digestion:**



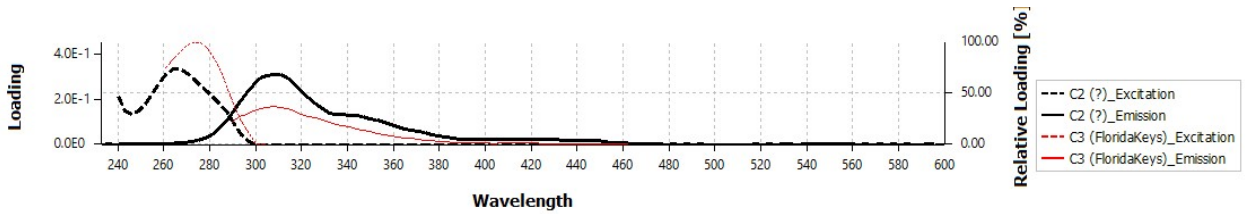
Matched Models: 12 / 70, Min Similarity Score: 0.97, Software: OpenFluor plugin for OpenChrom Version: 1.3.0.2017101902, Matched Components (Excitation/Emission)

c. Model Name: Anaerobic digestion

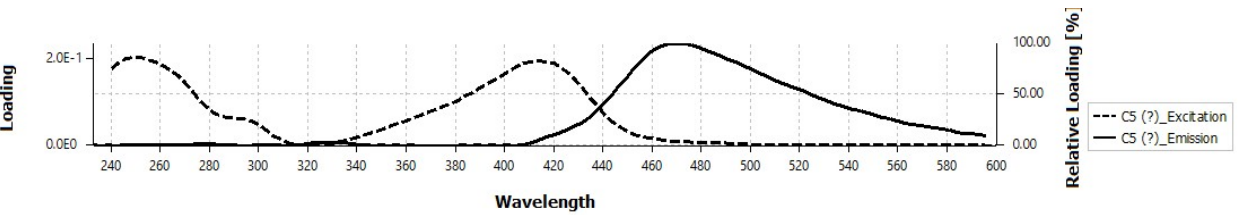
C1



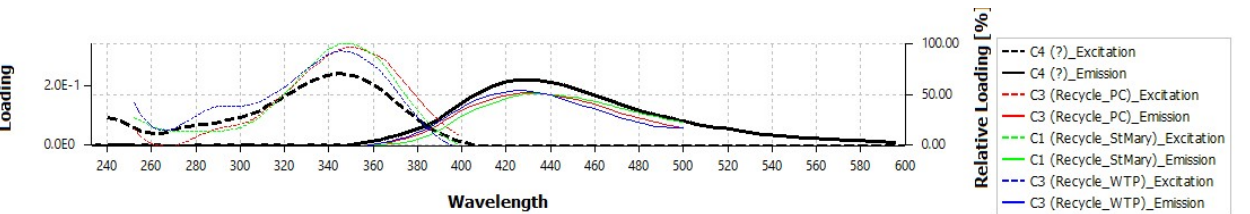
C2



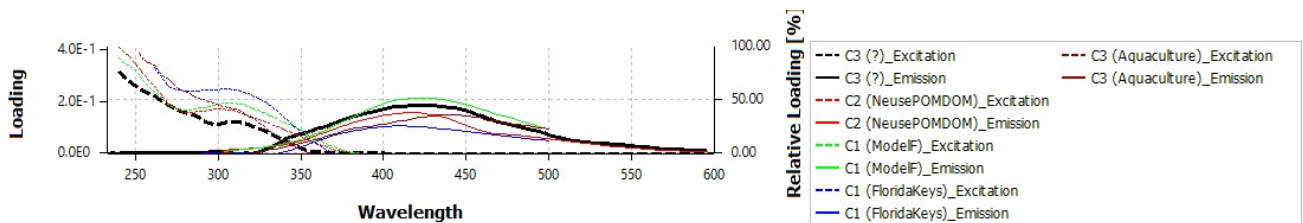
C3



C4



C5



Matched Models: 13 / 70

Min Similarity Score: 0.97

References of the Supplementary Materials:

1. S. Zmora-Nahum, O. Markovitch, J. Tarchitzky and Y. Chen, Dissolved organic carbon (DOC) as a parameter of compost maturity, *Soil Biology and Biochemistry*, 2005, **37**, 2109-2116.
2. K. Wang, W. Li, X. Gong, Y. Li, C. Wu and N. Ren, Spectral study of dissolved organic matter in biosolid during the composting process using inorganic bulking agent: UV-vis, GPC, FTIR and EEM, *International Biodeterioration & Biodegradation*, 2013, **85**, 617-623.
3. S. Hernandez-Ruiz, L. Abrell, S. Wickramasekara, B. Chefetz and J. Chorover, Quantifying PPCP interaction with dissolved organic matter in aqueous solution: Combined use of fluorescence quenching and tandem mass spectrometry, *Water Research*, 2012, **46**, 943-954.
4. A. Omoike, J. Chorover, K. D. Kwon and J. D. Kubicki, Adhesion of Bacterial Exopolymers to α -FeOOH: Inner-Sphere Complexation of Phosphodiester Groups, *Langmuir*, 2004, **20**, 11108-11114.
5. S. E. Cabaniss, Q. Zhou, P. A. Maurice, Y.-P. Chin and G. R. Aiken, A Log-Normal Distribution Model for the Molecular Weight of Aquatic Fulvic Acids, *Environ Sci Technol*, 2000, **34**, 1103-1109.
6. B. A. Poulin, J. N. Ryan and G. R. Aiken, Effects of Iron on Optical Properties of Dissolved Organic Matter, *Environ Sci Technol*, 2014, **48**, 10098-10106.
7. J. L. Weishaar, G. R. Aiken, B. A. Bergamaschi, M. S. Fram, R. Fujii and K. Mopper, Evaluation of specific ultraviolet absorbance as an indicator of the chemical composition and reactivity of dissolved organic carbon, *Environ Sci Technol*, 2003, **37**, 4702-4708.
8. J. Peuravuori and K. Pihlaja, Molecular size distribution and spectroscopic properties of aquatic humic substances, *Analytica Chimica Acta*, 1997, **337**, 133-149.
9. J. R. Helms, A. Stubbins, J. D. Ritchie, E. C. Minor, D. J. Kieber and K. Mopper, Absorption spectral slopes and slope ratios as indicators of molecular weight, source, and photobleaching of chromophoric dissolved organic matter, *Limnology and Oceanography*, 2008, **53**, 955-969.
10. C. A. Stedmon, S. Markager and H. Kaas, Optical properties and signatures of chromophoric dissolved organic matter (CDOM) in Danish coastal waters, *Estuar Coast Shelf S*, 2000, **51**, 267-278.
11. P. G. Coble, J. Lead, A. Baker, D. M. Reynolds and R. G. M. Spencer, in *Aquatic Organic Matter Fluorescence*, eds. P. G. Coble, J. Lead, A. Baker, D. M. Reynolds and R. G. M. Spencer, Cambridge University Press, Cambridge, 2014, pp. 75-122.
12. R. S. Gabor, Baker, A., McKnight, D. M., & Miller, M. P., Fluorescence indices and their interpretation., *Aquatic Organic Matter Fluorescence*, 2014, 303.
13. J. A. Korak, A. D. Dotson, R. S. Summers and F. L. Rosario-Ortiz, Critical analysis of commonly used fluorescence metrics to characterize dissolved organic matter, *Water Research*, 2014, **49**, 327-338.

14. R. B. Cattell, The Scree Test For The Number Of Factors, *Multivariate Behavioral Research*, 1966, **1**, 245-276.